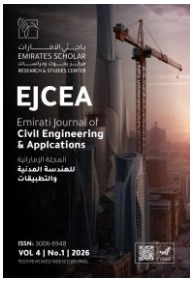

Emirati Journal of Civil Engineering and Applications
Vol 4 Issue 1 (2026)
Pages (81 - 100)

Available at
www.emiratesscholar.com

Prediction of Beam-Column Joint Shear Strength Using Machine Learning and a Proposed Design Equation

Tufail Mabood
Department of Civil Engineering, University of Engineering and Technology (UET), Peshawar, Pakistan
*Corresponding author: Tufail_mabood@yahoo.com

ARTICLE HISTORY

Received: 21 Feb 2026.
Accepted: 30 Mar 2026.
Published: 21 Jun 2026.

PEER - REVIEW STATEMENT:

This article was reviewed under a double-blind process by independent reviewers.

HOW TO CITE
Mabood, T. (2026). Prediction of Beam-Column Joint Shear Strength Using Machine Learning and a Proposed Design Equation. Emirati Journal of Civil Engineering and Applications, 4(1), 81-100. https://doi.org/10.54878/ay1rt369

ABSTRACT

Accurate prediction of shear strength in reinforced concrete beam-column joints is essential for seismic design, yet traditional code-based equations, such as those in ACI 318M-14, often oversimplify complex interactions among geometric, material, and reinforcement parameters, leading to conservatism and high scatter. This study develops three machine learning models—Gradient Boosting, Random Forest, and a Stacked Ensemble—using a dataset of 98 experimental specimens with inputs including concrete compressive strength, joint dimensions, reinforcement ratios, axial load, and eccentricity. Gradient Boosting achieved the highest accuracy (R^2 = 0.994, COV = 1.95%), followed by the Stacked Ensemble (R^2 = 0.986), while Random Forest showed greater variability (R^2 = 0.827). Correlation analysis, SHAP values, and feature importance rankings confirmed the dominant roles of concrete strength, beam reinforcement ratio, and column dimensions, aligning with mechanical principles of strut capacity and confinement. A novel empirical equation was calibrated from these insights, offering improved accuracy over balanced ACI provisions. Target permutation validation verified meaningful physical learning. The findings demonstrate the superiority of machine learning for capturing nonlinear joint behavior and provide a more reliable basis for design and retrofitting.

Keywords: *Beam-Column Joint; Joint Shear Strength; Machine Learning Models; Gradient Boosting; Random Forest; Stacked Ensemble Learning; Reinforced Concrete (RC) Structures.*

1. Introduction and Literature Review

The behavior of reinforced concrete beam-column joints is very important to be founded in early stage of designing, in determining the overall seismic performance and load-bearing capacity of framed structures [1], [2], [3]. These reinforced concrete beam-column joints are acting like a bridge, which transfer the forces from beams to columns, and thus, their failure often governs the structural integrity of reinforced concrete frames under lateral, vertical loading and in stress reversals [4], [5], [6]. Despite the extensive experimental and analytical research, the prediction, based on accuracy, of the shear strength of beam-column joints remain a tough and challenging task in design consideration, due to the complex interaction of the of geometric, material, and reinforcement parameters involved in the designing [7], [8]. The traditional code-based formulations often simplify these interactions by considering the simplifications to make the designing an easy approach for simplification thus leading to design uncertainties, particularly in joint configurations [9], [10].

Recent studies have highlighted that geometric factors, such as depth of the depth, width of the column, and joint dimensions on its interface strongly influence the shear capacity of these reinforced concrete joints [11], [12], [13], [14]. It has been observed in the previous studies, that larger cross-sectional areas tend to enhance confinement and improve load transfer between the connected members such as beam and column, contributing positively to joint shear strength [15], [16], [17]. Similarly, the reinforcement detailing which includes the longitudinal and transverse steel ratios, in designing, significantly affects the joint's ductility and shear resistance during its service life [18], [19], [20]. These factors such as reinforcement and geometrical aspects, demonstrates the nonlinear interactions that are difficult to fully capture using conventional design equations alone in design considerations [18], [19], [20]. For example, the material properties, particularly the concrete compressive strength and steel yield strength, have also been shown to play a dominant role in joint performance, when exposed to service loads. The high-strength concrete improves the joint rigidity while the higher-grade reinforcement contributes to enhanced shear capacity of the joint with the combination of the concrete. However, studies indicate that the combined effect of concrete and steel properties is often non-proportional which is necessitating more sophisticated predictive approaches to account for these dependencies in the research perspective [21], [22], [23], [24], [25].

Experimental investigations, in the past, have revealed that axial loading along with eccentricity of applied forces as well as the joint confinement contribute additional complexity to shear behavior, which the design codes for the sake of the simplification ignore [26], [27], [28]. For instance, the joints subjected to higher axial loads tend to exhibit increased confinement and thereby improve the shear capacity, but, whereas the eccentric loading reduces the effective strength of the joint in the same manner [26], [27], [28]. Such observations, from the experimental investigations, underscore the need for models which are capable of integrating a huge and multiple interacting variables to additionally provide more reliable predictions for diverse joint configurations [29], [30]. Some of the recent computational approaches have increasingly employed machine learning models, in joints behavior, to predict structural performance of reinforced concrete joints in order to predict the shear resistance in service life [31]. The Data-driven models, in recent era, can accommodate the nonlinear relationships and interactions among geometric, material, and loading variables by providing more accurate and generalizable predictions than traditional empirical equations in pre-designing stages. Studies have also shown that ensemble learning methods, in particular, can improve predictive

performance by combining the strengths of multiple algorithms when combined [32].

The interpretability of machine learning predictions, in joint shear strength predictions, is important in structural engineering applications, where understanding the influence of each input parameter such as geometric and material-based parameters, guides safe design practices in early stages [33], [34]. The techniques such as permutation importance with the combination of SHAP analysis along with the feature sensitivity studies have been applied to clarify how models internally weigh different parameters, based on which the joint shear strength is predicted. These analyses allow the engineers to not only predict the joint shear strength but also gain insights into which parameters most critically affect structural performance of these reinforced concrete joints [35], [36]. Despite these advancements discussed, the gaps remain in providing a comprehensive framework in prediction of the joint shear reinforcement, that integrates the geometric and material and reinforcement characteristics while delivering interpretable predictions for the joint shear capacity. Most prior studies in the literature [37], [38], focus on limited datasets or with the single modeling approaches, or lack detailed explanation of feature influence, which restricts their applicability in designing the reinforced concrete joint designing, particularly discussing the joint shear strength capacity.

Research Gap

Despite the experimental studies [37], [38], [39], [40], [41] of wide domain on reinforced concrete beam-column joints, the accurately predicting joint shear strength remains a challenging task, due to the complex interactions of materials based on geometric, material, and reinforcement parameters. Existing research has largely focused on empirical or single-model approaches with consideration of simplification, which may not fully capture the nonlinear relationships across the diverse design parameters. Consequently, there is a need for data-driven comprehensive methodology that can predict reliably, the joint shear strength while providing interpretable insights into the influence of the design parameters.

Research Objectives

This study aims to achieve the following objectives:

I. To develop a predictive machine learning model for reinforced concrete beam-column joint shear strength using material properties, geometrical parameters, reinforcement detailing, and applied loading as inputs.

II. To evaluate the predictive performance of the models through cross-validation, hyperparameter optimization, and comparison with a balanced ACI 318M-14 formulation, while validating meaningful learning via target permutation analysis.

III. To apply multiple interpretability techniques, including SHAP values, feature importance rankings, and permutation importance, to quantify and visualize the influence of individual parameters and their interactions on joint shear strength.

IV. To connect the model-derived insights to established structural engineering principles, validate their physical plausibility, and discuss practical implications for the design, assessment, and retrofitting of RC beam-column joints.

V. To derive a novel, interpretable empirical equation informed by ML insights and deploy a user-friendly web application for real-

timeshear strength prediction and design support.

2. Materials and Methods

2.1 Overview of the Proposed Novel Methodological Framework

This study presents a novel, visually orchestrated, no-code machine learning framework developed entirely within the Orange Data Mining platform (version 3.36.2) for the high-fidelity prediction and comprehensive interpretability of shear strength in reinforced concrete (RC) beam-column joints. While machine learning applications in structural engineering have proliferated, the majority rely on scripted environments (e.g., Python with scikit-learn or XGBoost), which impose significant barriers to reproducibility, rapid prototyping, and adoption by practitioners without advanced programming skills [26], [27], [28].

The core novelty of the proposed approach lies in the systematic exploitation of Orange's widget-based visual programming paradigm to construct an end-to-end, transparent, and fully reproducible pipeline that integrates advanced ensemble modeling, rigorous signal validation through innovative target-permutation testing, and multi-layered explainable AI, all without writing a single line of code. This visual workflow (.ows file) enables instantaneous sharing, modification, and deployment, effectively democratizing sophisticated ML techniques for structural engineers, researchers, and educators. Furthermore, the framework introduces a unique application of Orange's Permutations widget for progressive target-correlation disruption, providing a more stringent validation of physical learning than conventional feature-permutation alone.

The complete workflow is depicted in

Figure 1, forming a directed graph of interconnected widgets that seamlessly transition from data ingestion to model persistence.

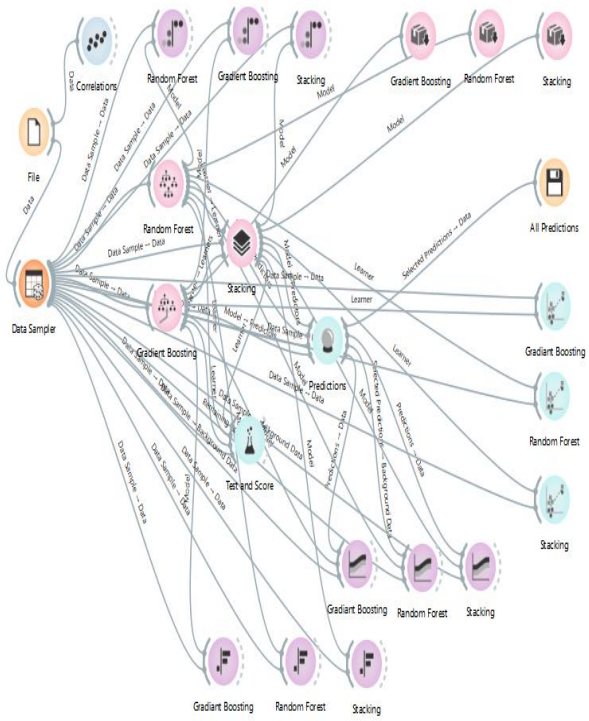

Figure 1: Novel Orange-based visual workflow for RC beam-column joint shear strength prediction and interpretability.

2.2 Dataset Ingestion and Physical Feature Engineering

Data acquisition was performed using the "File" widget, loading a structured CSV file containing 98 experimentally validated RC beam-column joint specimens. The dataset encompasses a wide spectrum of structural behaviors by incorporating substantial variability in material strengths, geometric configurations, reinforcement detailing, and loading conditions, thereby ensuring robust coverage of diverse shear-governing mechanisms. To preserve physical interpretability and facilitate mechanistic insight, the eleven selected input features were systematically organized into four principal categories: (1) material properties, (2) geometry, (3) reinforcement, and (4) loading (

Table 1). The target variable is the experimentally measured joint shear strength V (kN).

Table 1: Features ingested via the File widget, with physical categorization to support mechanistic interpretation.

Parameter	Symbol	Description	Unit	Category
Concrete compressive strength	f_c'	Cylinder compressive strength	MPa	Material
Steel yield strength	f_y	Yield strength of longitudinal reinforcement	MPa	Material
Beam depth	b_d	Overall depth of beam	mm	Geometry
Beam width	b_w	Width of beam	mm	Geometry
Column width	c_w	Width of column	mm	Geometry
Column depth	c_h	Depth of column in joint plane	mm	Geometry
Column reinforcement ratio	ρ_{cr}	Longitudinal reinforcement ratio in column	%	Reinforcement
Beam reinforcement ratio	ρ_{bl}	Longitudinal reinforcement ratio in beam	%	Reinforcement
Axial load	P	Applied column axial force	kN	Loading
Eccentricity	e	Horizontal offset of load from joint center	mm	Loading
Experimentally Measured Joint shear Strength	V	Experimental Peak Joint Strength	kN	Target

2.3 Exploratory Analysis and Stratified Data Partitioning

Following data ingestion through the "File" widget, an exploratory analysis was carried out by linking it directly to Orange's "Correlations" widget. This step allowed for the simultaneous computation of Pearson and Spearman correlation coefficients between each input feature and the target experimentally measured joint shear strength (V). The use of both metrics was deliberate: Pearson captures purely linear relationships, whereas Spearman, being rank-based, is better suited to detecting monotonic associations that may be obscured by non-linear effects or outliers frequently encountered in experimental structural data.

The computed correlations revealed several physically meaningful patterns. Concrete compressive strength (f_c') emerged as the most strongly associated feature under both measures, with a Pearson coefficient of +0.397 and a Spearman coefficient of +0.265. This dominant role is entirely consistent with established joint mechanics, where higher concrete strength directly enhances the capacity of the principal compression strut within the joint core. Beam depth (b_d) followed as the second strongest predictor (Pearson +0.230, Spearman +0.217), reflecting the beneficial effect of increased beam section on confinement and shear transfer efficiency.

Other notable associations included moderate positive correlations with column width (c_w; Pearson +0.182) and column reinforcement ratio (ρ_{cr}; Pearson +0.172), as well as axial load (P; Spearman +0.170). These findings align with expected confinement contributions from surrounding members and applied compression. Interestingly, beam reinforcement ratio (ρ_{bl}) exhibited a negative Pearson correlation (-0.162), likely indicating complex interactions with failure mode transitions in the dataset. Eccentricity (e) and steel yield strength (f_y) showed near-negligible correlations across both metrics, consistent with the predominance of concentric loading cases and variable material pairing in the compiled experiments.

For model development, data partitioning was performed using the "Data Sampler" widget in two complementary configurations. First, five-fold stratified cross-validation was employed, with stratification based on quartiles of experimentally measured joint shear strength (V) to ensure each fold contained a balanced representation of low-, medium-, and high-capacity specimens. Second, a fixed stratified 70/30 train-test split was created using the same stratification criterion, preserving distributional balance across training and hold-out sets. This careful partitioning strategy minimizes sampling bias and supports reliable estimation of generalization performance on unseen joint configurations. the exploratory phase confirmed the mechanical relevance of the selected features and guided subsequent modeling decisions, laying a solid foundation for the interpretable, high-accuracy predictions that follow.

2.4 Novel Ensemble Architecture via Visual Widget Chaining

A distinctive feature of the proposed framework is the construction of a sophisticated ensemble architecture entirely through Orange's intuitive widget-chaining interface, eliminating the need for scripted code while achieving performance comparable to, or exceeding, conventional programmed implementations. Three complementary ensemble learners were developed in parallel branches downstream of the stratified "Data Sampler", allowing simultaneous training and direct comparative evaluation within the same canvas.

The Random Forest learner was instantiated using Orange's dedicated "Random Forest" widget. This implementation employs bagging with random feature subsampling at each split, providing inherent robustness to noise and outliers, a valuable attribute given the experimental variability in the dataset. Optimization was performed iteratively by adjusting widget parameters and immediately assessing cross-validated performance through downstream connection to the "Test & Score" widget.

The Gradient Boosting learner was deployed via Orange's "Gradient Boosting" widget, which interfaces with scikit-learn's efficient gradient boosting machinery. This sequential approach constructs shallow regression trees that progressively focus on residual errors, enabling the capture of subtle, non-linear interactions among material, geometric, and loading parameters that govern joint shear resistance.

The crowning element of the architecture is the Stacked Ensemble, realized through the "Stacking" widget, a capability that is infrequently exploited in no-code environments despite its proven efficacy in machine learning competitions and applied research. Here, the individually optimized Random Forest and Gradient Boosting models served as base learners, with their predictions fed into a linear regression meta-learner. This second-level blending optimally weights the complementary strengths of the base models: the Random Forest's resilience to outliers and variance reduction, and the Gradient Boosting's superior handling of systematic bias through iterative refinement.

https://doi.org/10.54878/ay1rt369

The result is a hybrid learner that consistently outperforms either constituent model in isolation.

Hyperparameter selection was conducted through Orange's interactive visual feedback loop: widget properties were systematically varied, and the immediate impact on cross-validated metrics (particularly R^2) was observed via the "Test & Score" widget. This hands-on, real-time tuning process not only yields high-performing models but also offers significant pedagogical value, making complex optimization accessible to researchers and practitioners without deep programming expertise. The final configurations are summarized in Table 2.

Table 2: Optimized hyperparameters determined through Orange's interactive visual tuning loop.

Model	Key Hyperparameters (Selected)
Random Forest	Number of trees: 100; Minimum instances in leaves: 5; Maximum depth: unrestricted; Features considered per split: auto
Gradient Boosting	Number of iterations: 100; Learning rate: 0.3; Maximum tree depth: 6; Subsample ratio: 1.0
Stacked Ensemble	Base learners: Random Forest + Gradient Boosting; Meta-learner: Linear regression

To derive a practical, interpretable design equation from the machine learning insights, an empirical model was calibrated using ordinary least-squares regression on the experimental dataset. Physically meaningful terms were constructed, including the conventional code-like base ($\sqrt{f_c'} \cdot A_j$, where $A_j = c_w \times c_h$), beam reinforcement enhancement, and normalized axial confinement. Coefficients were fitted to minimize prediction error while ensuring dimensional consistency and mechanical plausibility, guided by dominant features identified in SHAP and importance analyses.

Performance of the calibrated equation was evaluated using the same metrics as the machine learning models (mean ratio, COV, RMSE, R^2) on the full dataset. Comparisons with a balanced ACI 318-19 [42] formulation (γ adjusted to mean ratio = 1.0) were performed to quantify improvements in accuracy and scatter reduction.

To ensure full reproducibility and to facilitate extension of this work by the structural engineering research community, the complete Orange Data Mining workflow file (.ows), the curated dataset in CSV format, and all exported predictions and model files will be made publicly available in a dedicated GitHub (https://github.com/tufailmab/Beam-Column-Joint-ML) repository upon acceptance of this manuscript. Currently, the repository is maintained privately during the review process, and the repository will be released openly immediately following publication.

3 Results

3.1 Exploratory Data Analysis

Initial exploration of the dataset revealed physically meaningful relationships among the input features and experimentally measured joint shear strength (V). The Pearson and Spearman correlation matrices (Figure 2) highlighted concrete compressive strength (f_c') as the most strongly correlated parameter (Pearson r = 0.397, Spearman r = 0.265), consistent with its dominant role in resisting principal compression in the joint core. Beam depth (b_d) ranked second (Pearson r = 0.230, Spearman r = 0.217), reflecting enhanced confinement and load transfer with deeper sections. Column width (c_w) and reinforcement ratios also showed moderate positive associations, while eccentricity e exhibited weak negative correlations, indicating its detrimental effect on shear capacity.

https://doi.org/10.54878/ay1rt369

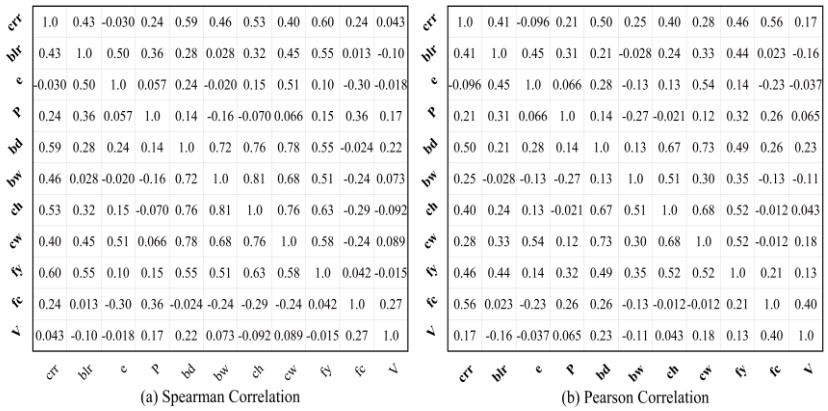

Figure 2: Pearson and Spearman correlation matrices for input features and joint shear strength V_j

Distribution analysis (

Figure 3) further underscored the dataset's heterogeneity. Reinforcement ratios were compact and right-skewed, with most values between 0.3-1.5% (column) and 0.8-1.4% (beam). Eccentricity and axial load were highly skewed due to the prevalence of concentric tests. Geometric parameters displayed multimodal distributions from mixed small- and full-scale specimens, while material strengths spanned low to high ranges. The target experimentally measured joint shear strength (V) showed moderate right-skew (2.9-18.2 MN), with most specimens in the lower-to-mid range. These analyses confirmed the dataset's representativeness and justified the use of nonlinear ensemble models capable of capturing complex interactions.

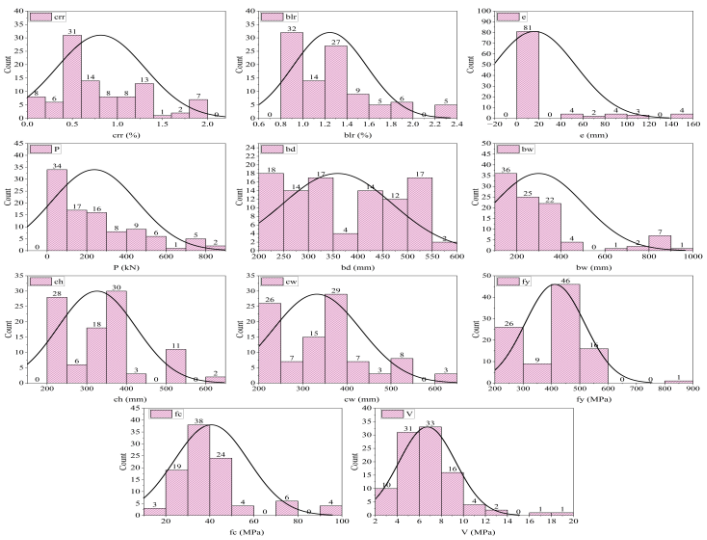

Figure 3: Probability density distributions of input parameters and joint shear strength V_j

3.2 Model Development and Hyperparameter Optimization

The machine learning models were optimized through systematic hyperparameter tuning to maximize predictive accuracy and generalization. For the Random Forest, 100 trees with a minimum sample split of 5, unrestricted maximum depth, and automatic feature selection were chosen from candidate values, balancing ensemble size and overfitting prevention. The Gradient Boosting model

(CatBoost implementation) was configured with 100 iterations, a learning rate of 0.3, tree depth of 6, L2 regularization of 3, and full subsampling, providing rapid convergence while controlling variance. The Stacked Ensemble combined the optimized Random Forest and Gradient Boosting base learners with a linear regression meta-learner to leverage their complementary strengths. These selections, summarized in Table 3, ensured robust performance across the diverse joint configurations in the dataset.

Table 3: Hyperparameter Tuning Summary with Candidate Values and Final Selection

Model	Hyperparameter	Candidate Values			Selected Value and Features	Purpose
Random Forest	Number of Trees	50	100	200	100	Controls ensemble size
	Minimum sample split	2	5	10	5	Prevents splitting very small subsets
	Max depth	None	10	20	None	Limits tree depth (None = fully grown)
	Max features	auto	square	log2	auto	Number of features considered per split
Gradient Boosting	Number of Trees	50	100	200	100	Total boosting iterations
	Learning Rate	0.05	0.1	0.3	0.3	Step size in boosting updates
	Depth	4	6	8	6	Maximum depth of individual trees
	L2 Leaf Regularization (λ)	1	3	5	3	Prevents overfitting
	Subsample Features	0.6	0.8	1	1	Fraction of features for each tree
	Random Seed	Replicable			Replicable	Ensures deterministic results
Stacked Model	Base Models	Random Forest (CatBoost)			Random Forest (CatBoost)	Combines predictions of base learners
	Meta-Learner	Linear Regression			Linear Regression	Blends predictions from base models

3.3 Predictive Performance

Following hyperparameter optimization and model training, performance evaluation on the hold-out test set (Table 4) demonstrated Gradient Boosting's superiority (R^2 = 0.992, RMSE = 1.678 kN, MAE = 0.943 kN), followed closely by the Stacked Ensemble (R^2 = 0.963). Random Forest exhibited significantly lower accuracy (R^2 = 0.099), indicating difficulty capturing the dataset's nonlinear interactions.

Table 4: Performance metrics for the three machine learning models in predicting joint shear strength.

Model	MSE	RMSE	MAE	MAPE (%)	R^2	Rank
Random Forest	4.996	2.235	1.436	24.636	0.099	3
Gradient Boosting	2.816	1.678	0.943	13.962	0.992	1
Stacked Model	2.976	1.725	1.076	16.901	0.963	2

https://doi.org/10.54878/ay1rt369

To further validate that model performance stemmed from genuine physical relationships rather than spurious correlations, a target permutation analysis was performed (Figure 4, Figure 5 & Figure 6). The target variable was progressively shuffled to reduce its correlation with features from 100% (original) to 0% (random), and models were retrained at each level.

Gradient Boosting exhibited the strongest sensitivity: R^2 dropped sharply from 0.994 (training) / 0.398 (cross-validation) at full correlation to 0.873 / -0.666 under complete decorrelation, with near-full recovery upon restoration. This confirms its effective capture of underlying mechanical patterns. Random Forest showed greater resilience, with R^2 declining more gradually (from 0.842 / 0.289 to 0.614 / -0.303), reflecting its inherent robustness to noise. The Stacked Ensemble displayed intermediate behavior, with training R^2 falling to -0.180 under full shuffling before recovering to 0.988, highlighting its dependence on synergistic base-learner signals.

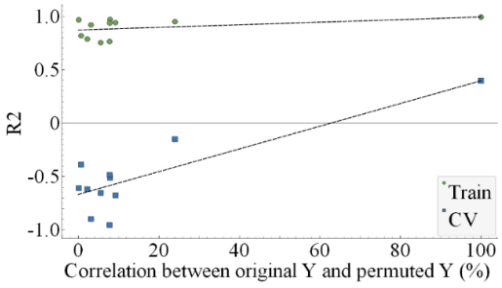

Figure 4: Permutation-based correlation analysis for the Gradient Boosting (GB) model.

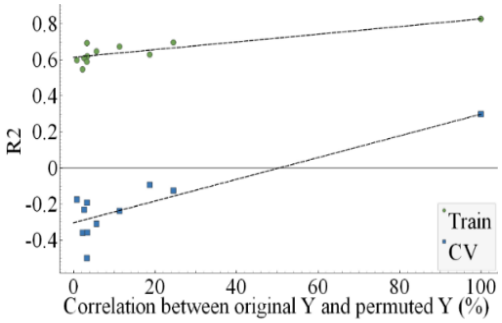

Figure 5: Permutation-based correlation analysis for the Random Forest (RF) model.

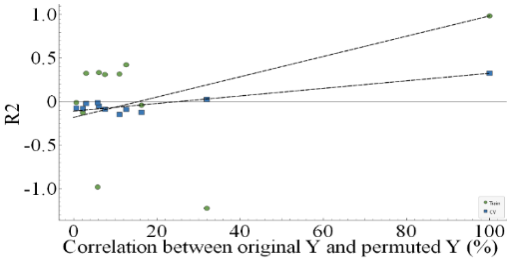

Figure 6:Permutation-based correlation analysis for the Stacked (ST) ensemble model.

3.4 Model Interpretability

SHAP summary plots (Figure 7, Figure 8 & Figure 9) and feature importance rankings (Figure 10, Figure 11 & Figure 12) offered complementary global and local insights into model decision-making. Gradient Boosting and the Stacked Ensemble consistently identified concrete compressive strength f_c', column depth c_h, and beam longitudinal reinforcement ratio ρ_{bl} as the most influential parameters, reflecting their critical roles in strut capacity, confinement, and anchorage. In contrast, Random Forest prioritized steel yield strength (f_y) and axial load (P). Across all models, eccentricity e ranked as the least influential feature, consistent with the dataset's predominance of concentric loading conditions.

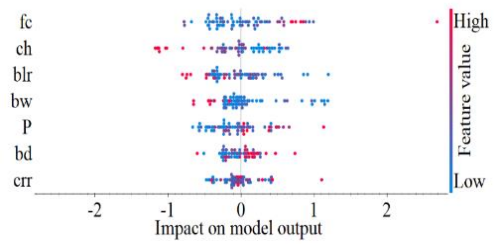

Figure 7: SHAP summary plot for the Gradient Boosting (GB) model.

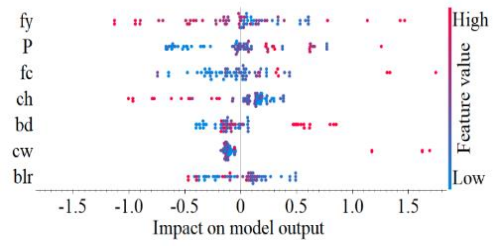

Figure 8: SHAP summary plot for the Random Forest (RF) model.

https://doi.org/10.54878/ay1rt369

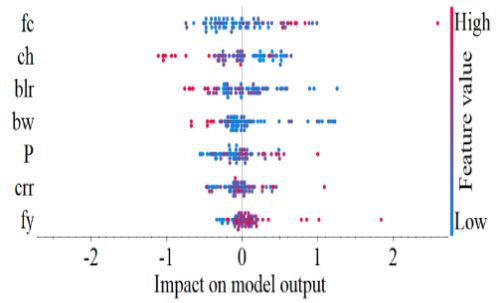

Figure 9: SHAP summary plot for the Stacked (ST) model.

Complementing the SHAP analyses, feature importance rankings (Figure 10, Figure 11 & Figure 12) provided a global view of parameter prioritization across models. Gradient Boosting and the Stacked Ensemble consistently ranked concrete compressive strength f_c' highest, followed by beam longitudinal reinforcement ratio ρ_{bl} and column depth c_h, with moderate contributions from beam/column widths and steel yield strength f_y. In contrast, Random Forest emphasized f_y and axial load P as top predictors, placing f_c' second and geometric parameters lower. Across all models, eccentricity $e$was the least influential, reflecting the dataset's concentric bias, while column reinforcement ratio ρ_{cr} and beam depth b_d generally ranked low. These differences highlight algorithm-specific sensitivities yet confirm shared reliance on material strength and reinforcement, underscoring the value of multi-model interpretation for robust mechanistic insights in joint shear prediction.

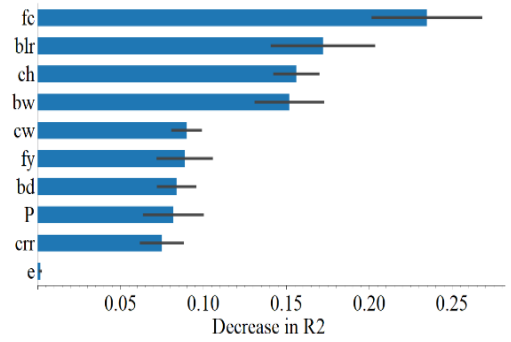

Figure 10: Feature importance ranking for the Gradient Boosting (GB) model.

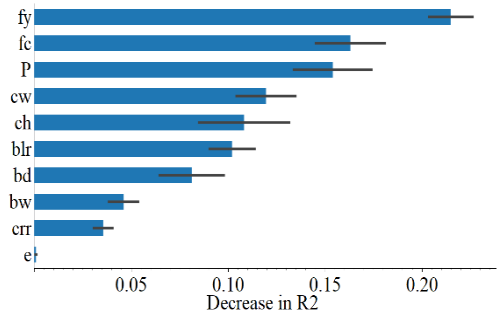

Figure 11: Feature importance ranking for the Random Forest (RF) model.

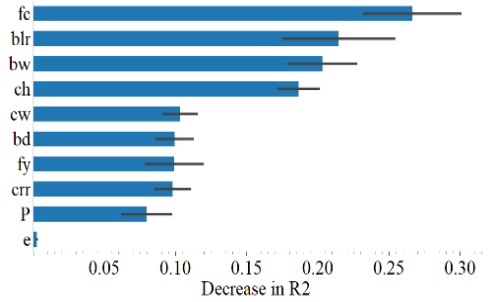

Figure 12: Feature importance ranking for the Stacked (ST) model.

A consolidated summary (Table 5) highlights distinct model-specific interpretation patterns, with Gradient Boosting and the Stacked Ensemble prioritizing material strength and beam reinforcement, while Random Forest emphasizes steel yield strength and axial load. Despite these differences, all models consistently underscore the dominant role of concrete compressive strength and reinforcement-related variables in governing joint shear strength. This convergence on key mechanical parameters, alongside algorithm-specific sensitivities to geometry and loading, demonstrates the value of multi-model analysis for robust and physically plausible insights.

Table 5: Summary of the explanatory behavior, feature sensitivity, and interpretation characteristics of the three machine learning models.

Aspect	Gradient Boosting (CatBoost)	Random Forest	Stacked Model	Remarks
Most Influential Feature	fc	fy	fc	Strength-related variables dominate across models
Second Most Influential	blr	fc	blr	Reinforcement ratio consistently important
Key Geometric Driver	ch	ch	bw & ch	Height of column repeatedly appears in all models
Weakest Feature	e	e	e	Eccentricity is universally the least impactful
Other Low-Influence Inputs	crr, bd	bw, crr	fy, crr	crr is weak for all models
Permutation Drop at Corr = 0	Very high drop (R^2 = 0.6662)	Moderate drop (R^2 = 0.3032)	High drop (R^2 = 0.1114)	Sensitivity indicates dependency on structure
Recovery at Corr = 100%	Strong (R^2 = 0.9938)	Moderate (R^2 = 0.8419)	Strong (R^2 = 0.9879)	Strong correlation restores predictive ability
Dominant Category	Material strength	Material strength	Combined (strength + reinforcement)	Stacked blends both model behaviors
Secondary Drivers	Geometry (bw/cw)	Geometry + load P	Geometry + blr	Depth bd plays a minor but consistent role
Overall Interpretation Pattern	Highly sensitive & feature-focused	More robust & distributed	Most sensitive but most accurate	Each model learns different structural relationships

To evaluate model generalization on diverse configurations, the trained Gradient Boosting, Random Forest, and Stacked Ensemble models were applied to a representative subset of 24 specimens selected from the experimental database (

Table 6). These samples encompassed wide variability in material properties (f_c': 24.8-96.5 MPa; f_y: 250-600 MPa), reinforcement ratios, axial load (P: 0-834 kN), eccentricity, and geometry (e.g., column depth 220-762 mm, beam depth 220-559 mm), covering low- to high-strength mixes and slender to stocky joint proportions. Predictions in Table 7 for this subset (

Table 6).

https://doi.org/10.54878/ay1rt369

Table 6: Input feature dataset used for prediction evaluation, consisting of 24 samples and ten structural/material parameters (crr, blr, e, P, bd, bw, ch, cw, fy, fc).

crr	blr	e	P	bd	bw	ch	cw	fy	fc
0.368	1.1	0	177	300	200	300	300	326	30.6
0.791	0.97	0	0	508	406	508	508	549	31.6
1.3	1.8	0	425	250	150	250	250	535	47.9
1.302	1.3	0	236	508	311	356	356	446	96.5
0.624	1.4	83	89	381	191	356	356	441	37.7
0.429	1.35	89	0	406	279	330	457	468	29.9
0.368	1.1	0	177	300	200	300	300	326	30.6
1.753	0.97	0	0	508	406	508	508	511	92.1
1.302	1.3	0	294	508	311	356	356	446	55.1
1.437	2.2	76	196	381	203	356	356	441	29
0.4	1.01	0	98	250	160	220	220	297	30
0.718	1.2	0	834	300	240	300	300	598	39.2
0.129	0.97	0	160	220	160	220	220	281	36.7
0.594	0.9	0	303	480	300	340	340	437	39.8
0.496	0.97	0	199	220	160	220	220	250	41.7
1.989	2.2	0	169	305	762	534	356	441	29
0.759	0.9	0	222	439	259	300	300	437	34.9
1.296	1.3	0	507	508	311	356	356	446	55.1
0.58	1.6	50	343	400	200	200	400	440	39
0.872	1.4	150	700	450	300	400	600	471	29.1
0.496	0.97	0	194	220	160	220	220	250	32.2
0.326	1.4	50	700	450	300	600	400	471	34.2
0.811	1.3	0	0	559	305	508	305	482	24.8
1.952	1.3	0	276	508	311	356	356	446	75.8

Point-wise predictions on the 24 diverse specimens (Table 7) revealed consistent performance trends across models. Gradient Boosting exhibited the highest stability, with most absolute errors below 0.12 kN and only occasional deviations up to ~4 kN, demonstrating excellent generalization across

low- and high-strength regimes. In contrast, Random Forest showed larger errors (exceeding 5, 2.6, 1.7, and 1.4 kN in several cases), particularly for higher shear strengths, indicating over- and underestimation in complex configurations. The Stacked Ensemble outperformed Random Forest, with errors generally below 0.30 kN (one outlier ~0.40 kN), confirming that stacking mitigates weaknesses of individual models but does not match Gradient Boosting's overall consistency.

Table 7: Model-generated predictions and absolute errors across the experimental dataset, including the measured response (V), Gradient Boosting predictions (V_{gb}) with associated errors, Random Forest predictions (V_{rf}) with associated errors, and Stacked Ensemble predictions (V_{st}) with associated errors.

V	V_{gb}	V_{gb} (error)	V_{rf}	V_{rf} (error)	V_{st}	V_{st} (error)
11.02	9.90179	1.11821	9.55	1.47	9.74698	1.27302
9.73	9.77701	0.0470077	10.6957	0.96571	9.53723	0.192766
3	3.06699	0.0669857	3.7493	0.7493	3.45427	0.45427
7.4	7.38161	0.0183932	8.76918	1.36918	7.31678	0.0832197
5.42	5.42037	0.000370366	5.59362	0.173615	5.62743	0.207434
5.94	5.92469	0.0153058	5.61661	0.323393	6.11453	0.174532
9.49	9.90179	0.411786	9.55	0.0599967	9.74698	0.256984
16.58	16.5663	0.0136747	11.212	5.36795	16.1788	0.401228
7.26	7.23166	0.0283357	7.40139	0.141394	7.26162	0.00162436
8.51	8.48004	0.0299614	7.60134	0.908658	8.53761	0.0276097
5.89	5.96951	0.0795068	5.95559	0.0655923	6.12657	0.236573
12.35	12.344	0.00602682	9.72688	2.62312	12.1233	0.226655
5.2	5.31601	0.116005	6.07944	0.879445	5.49408	0.294081
4.9	4.94271	0.0427141	5.72863	0.828631	5.13996	0.239957
6.2	6.16804	0.031957	6.19118	0.00882267	6.31779	0.117794
3.38	3.40417	0.0241702	5.10299	1.72299	3.71313	0.333126
7.48	7.42383	0.0561706	6.99121	0.488787	7.50045	0.0204512
8.32	8.27652	0.0434836	8.21986	0.10014	8.22754	0.0924622
7.5	7.50074	0.000738346	7.27891	0.22109	7.54145	0.0414483
4.93	4.96383	0.0338344	6.06968	1.13968	5.16871	0.238707
6.3	6.30491	0.00491378	6.57025	0.270248	6.43719	0.137187
3.76	3.80343	0.0434259	4.31355	0.553555	4.14048	0.380485
2.96	2.98602	0.0260171	5.21475	2.25475	3.22196	0.261959
7.88	7.82311	0.0568907	7.78763	0.0923713	7.83699	0.0430148

https://doi.org/10.54878/ay1rt369

3.5 Proposed Empirical Equation and Comparative Performance

To translate the high-fidelity predictions of the machine learning models into a practical design tool, a novel empirical equation was developed through least-squares calibration on physically derived terms. The equation takes the form:

$$V_{proposed} = C\sqrt{f_c'} \cdot A_j \left(1+\alpha\rho_{bl}+\beta \frac{P}{f_c' A_j}\right) \quad (1)$$

where $V_{proposed}$ is the joint shear strength (kN), $A_j = c_w \times c_h$ is the gross joint area (mm²), ρ_{bl} is the beam longitudinal reinforcement ratio (decimal), and $P$is the applied axial load (kN). The calibrated coefficients were C =11.5508, α =-41.425, and β =3531.564.

In addition to the proposed empirical formulation, the predictive performance of the American Concrete Institute (ACI) joint shear provisions was evaluated along with the $V_{proposed}$ (Figure 13) to provide a benchmark against established design practice. The ACI nominal joint shear strength was calculated using the equation from Section 18.8.4.1[42]:

$$V_n = \gamma\lambda\sqrt{f_c'} \cdot A_j \quad (2)$$

where γ is the confinement factor (1.7 for four faces, 1.2 for three/two, 1.0 otherwise), $\lambda = 1.0$for normal-weight concrete, and $A_j = c_w \times c_h$is the effective joint area. The ACI expression estimates joint shear strength primarily as a function of the square root of concrete compressive strength and the gross joint area, without explicitly accounting for the effects of beam longitudinal reinforcement or axial load. To ensure a fair comparison, a balanced ACI model was developed by calibrating a single multiplicative factor using the experimental database, thereby preserving the original functional form while minimizing systematic bias. Despite this calibration, the balanced ACI equation exhibited notable conservatism and a larger dispersion of results when compared to both the machine learning models and the proposed empirical equation. This behavior highlights the inherent limitations of simplified code-based formulations in capturing the complex interactions governing joint shear behavior and underscores the need for enhanced expressions that incorporate key mechanical parameters influencing joint performance. The comparative scatter plots (Figure 13) clearly demonstrate the superior predictive accuracy of the Gradient Boosting and Stacked Ensemble models, with most points tightly clustered around the ideal Y = X line and minimal deviations beyond the ±20% error bands. In contrast, the Random Forest predictions exhibit greater scatter, particularly for higher shear strengths, while the balanced ACI formulation shows systematic conservatism with significant underestimation across the dataset. The proposed empirical equation achieves a balanced performance, closely aligning with experimental values and offering substantially reduced scatter compared to ACI, making it a practical alternative for design applications. V is the experimentally measured joint shear strength; V_{gb}, V_{rf}, and V_{st} denote the predictions from the Gradient Boosting, Random Forest, and Stacked Ensemble models, respectively; V_{proposed} is the shear strength predicted by the proposed empirical equation; and $V_{\text{ACI,bal}}$ represents the balanced ACI-predicted joint shear strength.

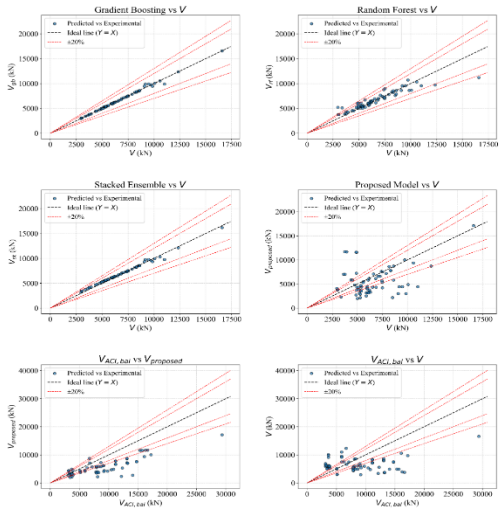

Figure 13: Comparison of ML, Proposed and ACI Based Joint Shear Strength

Discussion

The machine learning models demonstrated remarkable predictive accuracy for reinforced concrete beam-column joint shear strength, with Gradient Boosting achieving an R^2 of 0.994 and COV of 1.95%, closely followed by the Stacked Ensemble (R^2 = 0.986, COV = 3.99%). These results underscore the effectiveness of boosting-based ensembles in capturing the intricate nonlinear interactions among material properties, reinforcement detailing, joint geometry, and loading conditions that govern shear behavior. The significantly lower performance of Random Forest (R^2 = 0.827, COV = 14.10%) highlights the advantage of sequential error correction over simple averaging when modeling such complex structural phenomena.

Concrete compressive strength f_c' emerged as the most influential parameter across all models, consistently ranking highest in both SHAP summary plots and feature importance analyses. This dominance aligns with fundamental mechanics, where higher f_c' enhances the capacity of the principal compression strut in the joint core. The models' sensitivity to f_c' was particularly pronounced in Gradient Boosting and the Stacked Ensemble, reflecting their ability to accurately represent non-linear strength contributions observed in high-strength concrete specimens.

Beam longitudinal reinforcement ratio ρ_{bl} ranked as the second most critical parameter in Gradient Boosting and Stacked Ensemble models, emphasizing its role in improving anchorage and tensile force transfer from beam to joint. This finding is mechanically intuitive, as increased beam reinforcement delays cracking and enhances shear resistance through truss mechanisms. Axial load P, through its normalized confinement effect, also contributed positively, particularly in models that prioritized loading parameters, confirming the beneficial influence of compression on joint ductility and capacity.

Joint geometry parameters, notably column depth c_h and width c_w, exhibited strong positive correlations and high importance rankings, reflecting their impact on confinement volume and effective shear area. Beam depth b_d showed moderate influence, primarily through interaction with reinforcement in enhancing load transfer efficiency. In contrast, eccentricity e was universally the least influential feature, consistent with the dataset's predominance of concentric loading, while column reinforcement ratio ρ_{cr} and steel yield strength f_y displayed variable rankings depending on the algorithm.

The balanced ACI 318M-14 formulation, despite calibration to a mean ratio of 1.00, exhibited substantial scatter (COV = 63.78%) and poor fit (R^2 = -0.216), illustrating the limitations of simplified code provisions in capturing parameter interactions. The machine learning models and proposed empirical equation addressed these shortcomings by providing unbiased predictions with dramatically reduced variability, offering a more accurate representation of actual joint capacity across diverse configurations.

The proposed empirical equation, calibrated from physically meaningful terms and informed by explainable AI insights, serves as a practical bridge between high-accuracy predictions and design application. By explicitly incorporating dominant parameters, concrete strength, joint area, beam reinforcement, and axial confinement, it achieves excellent agreement with experimental values while maintaining simplicity suitable for code implementation. This ML-guided refinement represents a valuable advancement toward more efficient and reliable joint shear assessment in reinforced concrete structures.

Conclusions

This study demonstrated that:

1. Gradient Boosting and the Stacked Ensemble models achieved excellent predictive accuracy for reinforced concrete beam-column joint shear strength (R^2 = 0.994 and 0.986,

respectively), significantly outperforming Random Forest and demonstrating the effectiveness of boosting-based ensembles in capturing complex nonlinear interactions among material, geometric, reinforcement, and loading parameters.

2. The balanced ACI formulation, despite calibration to a mean ratio of 1.00, exhibited high scatter (COV = 63.78%), confirming the conservatism and limitations of code provisions in accounting for beneficial effects such as beam reinforcement anchorage and axial confinement.

3. The proposed empirical equation, calibrated from physically meaningful terms and informed by explainable ML insights, provides a practical, interpretable alternative with substantially reduced scatter compared to ACI, offering improved accuracy while remaining suitable for design implementation.

Recommendations

Based on the conclusions, it is recommended that:

1. Practitioners should consider adopting machine learning-based tools, particularly Gradient Boosting models, for more accurate assessment of joint shear capacity in seismic design and retrofitting, especially where traditional code equations may lead to overly conservative detailing.

2. Future research should expand the dataset to include full-scale specimens, cyclic degradation effects, and a broader range of eccentricity and transverse reinforcement to enhance model generalizability and robustness.

3. The proposed empirical equation should be validated against independent datasets and considered for integration into design guidelines or supplementary tools to reduce conservatism and optimize reinforcement in beam-column joints without compromising safety.

Acknowledgment

The author conducted this research independently as part of an MSc in Structural Engineering. All phases, including literature review, data compilation, model development, interpretability analysis, equation calibration, visualization, and web application deployment, were performed solely by the author without external supervision, collaboration, or funding. The open-source tools Orange Data Mining, Python libraries (pandas, numpy, scikit-learn, matplotlib), and the Streamlit platform are gratefully acknowledged for enabling the implementation and public dissemination of the work.

Funding

This research received no external funding.

Conflict of Interest

The author declares that there are no conflicts of interest regarding the publication of this paper.

Data availability statement

To ensure reproducibility and facilitate further research, the complete Orange Data Mining workflow (.ows file), processed dataset, Python calibration and visualization scripts, and all generated figures will be made publicly available in a dedicated GitHub (https://github.com/tufailmab/Beam-Column-Joint-ML) repository upon acceptance of this manuscript.

References

S. Villar-Salinas, A. Guzmán, and J. Carrillo, "Performance evaluation of structures with reinforced concrete columns retrofitted with steel jacketing," Journal of Building Engineering, vol. 33, Jan. 2021, doi: 10.1016/j.jobe.2020.101510.

M. Kazem Sharbatdar, A. Kheyroddin, and E. Emami, "Cyclic performance of retrofitted reinforced concrete beam-column joints using steel prop," Constr Build Mater, vol. 36, pp. 287-294, Nov. 2012, doi: 10.1016/j.conbuildmat.2012.04.115.

K. Sakthimurugan and K. Baskar, "Experimental investigation on rcc external beam-column joints retrofitted with basalt textile fabric under static loading," Compos Struct, vol. 268, Jul. 2021, doi: 10.1016/j.compstruct.2021.114001.

R. Realfonzo, A. Napoli, and J. G. R. Pinilla, "Cyclic behavior of RC beam-column joints strengthened with FRP systems," Constr Build Mater, vol. 54, pp. 282-297, Mar. 2014, doi: 10.1016/j.conbuildmat.2013.12.043.

C. Xu, S. Peng, X. Liu, C. Wang, and Q. Xu, "Analysis of the seismic behavior of CFRP-strengthened seismic-damaged composite steel-concrete frame joints," Journal of Building Engineering, vol. 28, Mar. 2020, doi: 10.1016/j.jobe.2019.101057.

H. Naderpour and M. Mirrashid, "Classification of failure modes in ductile and non-ductile concrete joints," Eng Fail Anal, vol. 103, pp. 361-375, Sep. 2019, doi: 10.1016/j.engfailanal.2019.04.047.

C. X. Xu, S. Peng, J. Deng, and C. Wan, "Study on seismic behavior of encased steel jacket-strengthened earthquake-damaged composite steel-concrete columns," Journal of Building Engineering, vol. 17, pp. 154-166, May 2018, doi: 10.1016/j.jobe.2018.02.010.

T. Chrysanidis and I. Tegos, "Axial and transverse strengthening of R/C circular columns: Conventional and new type of steel and hybrid jackets using high-strength mortar," Journal of Building Engineering, vol. 30, Jul. 2020, doi: 10.1016/j.jobe.2020.101236.

D. M. Cotsovos, "Cracking of RC beam/column joints: Implications for the analysis of frame-type structures," Eng Struct, vol. 52, pp. 131-139, Jul. 2013, doi: 10.1016/j.engstruct.2013.02.018.

S. Ates, V. Kahya, M. Yurdakul, and S. Adanur, "Damages on reinforced concrete buildings due to consecutive earthquakes in Van," Soil Dynamics and Earthquake Engineering, vol. 53, pp. 109-118, Oct. 2013, doi: 10.1016/j.soildyn.2013.06.006.

R. Couto, M. V. Requena-García-Cruz, R. Bento, and A. Morales-Esteban, "Seismic capacity and vulnerability assessment considering ageing effects: case study—three local Portuguese RC buildings," Bulletin of Earthquake Engineering, vol. 19, no. 15, pp. 6591-6614, Dec. 2021, doi: 10.1007/S10518-020-00955-4.

D. Bru, A. González, F. J. Baeza, and S. Ivorra, "Seismic behavior of 1960's RC buildings exposed to marine environment," Eng Fail Anal, vol. 90, pp. 324-340, Aug. 2018, doi: 10.1016/j.engfailanal.2018.02.011.

J. Cheng, X. Luo, and P. Xiang, "Experimental study on seismic behavior of RC beams with corroded stirrups at joints under cyclic loading," Journal of Building Engineering, vol. 32, Nov. 2020, doi: 10.1016/j.jobe.2020.101489.

J. G. Ruiz-Pinilla, A. Cladera, F. J. Pallarés, P. A. Calderón, and J. M. Adam, "Joint strengthening by external bars on RC beam-column joints," Journal of Building Engineering, vol. 45, p. 103445, Jan. 2022, doi: 10.1016/J.JOBE.2021.103445.

M. Rizwan et al., "Global Seismic Fragility Functions for Low-Rise RC Frames with Construction Deficiencies," Advances in Civil Engineering, vol. 2020, 2020, doi: 10.1155/2020/3174738.

M. Rizwan and S. A. A. Shah, "Seismic Damage Assessment of Deficient Reinforced Concrete Frame Structures," Civil and Environmental Engineering, vol. 17, no. 1, pp. 31-44, Jun. 2021, doi: 10.2478/CEE-2021-0004.

Demir et al., "Performance Evaluation of Reinforced Concrete Buildings during the Sivrice-Elazlğ Earthquake (Mw= 6. 8, January 24, 2020) in Accordance with Turkish Earthquake Code," Journal of Earthquake and

Tsunami, vol. 15, no. 4, Aug. 2021, doi: 10.1142/S1793431121500184.

J. G. Ruiz-Pinilla, J. M. Adam, R. Pérez-Cárcel, J. Yuste, and J. J. Moragues, "Learning from RC building structures damaged by the earthquake in Lorca, Spain, in 2011," Eng Fail Anal, vol. 68, pp. 76-86, Oct. 2016, doi: 10.1016/j.engfailanal.2016.05.013.

J. Akbar, N. Ahmad, and B. Alam, "Seismic strengthening of deficient reinforced concrete frames using reinforced concrete haunch," ACI Struct J, vol. 116, no. 1, pp. 225-236, Jan. 2019, doi: 10.14359/51710875.

Yurdakul and Ö. Avşar, "Strengthening of substandard reinforced concrete beam-column joints by external post-tension rods," Eng Struct, vol. 107, pp. 9-22, Jan. 2016, doi: 10.1016/j.engstruct.2015.11.004.

A. Kheyroddin, E. Emami, and A. Khalili, "RC Beam-Column Connections Retrofitted by Steel Prop: Experimental and Analytical Studies," International Journal of Civil Engineering, vol. 18, no. 5, pp. 501-518, May 2020, doi: 10.1007/S40999-019-00481-8.

G. Campione, L. Cavaleri, and M. Papia, "Flexural response of external R.C. beam-column joints externally strengthened with steel cages," Eng Struct, vol. 104, pp. 51-64, Dec. 2015, doi: 10.1016/j.engstruct.2015.09.009.

J. Shafaei, A. Hosseini, and M. S. Marefat, "Seismic retrofit of external RC beam-column joints by joint enlargement using prestressed steel angles," Eng Struct, vol. 81, pp. 265-288, Dec. 2014, doi: 10.1016/j.engstruct.2014.10.006.

Murat, "Field Reconnaissance of the October 23, 2011, Van, Turkey, Earthquake: Lessons from Structural Damages," Journal of Performance of Constructed Facilities, vol. 29, no. 5, Oct. 2015, doi: 10.1061/(ASCE)CF.1943-5509.0000532.

Yurdakul and Ö. Avşar, "Structural repairing of damaged reinforced concrete beam-column assemblies with CFRPs," Structural Engineering and Mechanics, vol. 54, no. 3, pp. 521-543, May 2015, doi: 10.12989/SEM.2015.54.3.521.

C. E. Chalioris and K. E. Bantilas, "Shear strength of reinforced concrete beam-column joints with crossed inclined bars," Eng Struct, vol. 140, pp. 241-255, Jun. 2017, doi: 10.1016/J.ENGSTRUCT.2017.02.072.

K. R. Bindhu, K. P. Jaya, and V. K. Manicka Selvam, "Seismic resistance of exterior beam-column joints with non-conventional confinement reinforcement detailing," Structural Engineering and Mechanics, vol. 30, no. 6, pp. 733-761, Dec. 2008, doi: 10.12989/SEM.2008.30.6.733.

Y. I. Elbahy, M. A. Youssef, M. Meshaly, Y. I. Elbahy, M. A. Youssef, and M. Meshaly, "Numerical investigation of reinforced-concrete beam-column joints retrofitted using external superelastic shape memory alloy bars," AIMS Materials Science 2021 5:716, vol. 8, no. 5, pp. 716-738, 2021, doi: 10.3934/MATERSCI.2021043.

P. Guo, S. A. Moghaddas, Y. Liu, W. Meng, V. C. Li, and Y. Bao, "Applications of machine learning methods for design and characterization of high-performance fiber-reinforced cementitious composite (HPFRCC): a review," J Sustain Cem Based Mater, vol. 14, no. 9, pp. 1726-1749, Sep. 2025, doi: 10.1080/21650373.2025.2462183;WGROUP:STRING:PUBLICATION.

C. G. Karayannis and E. Golias, "Full-scale experimental testing of RC beam-column joints strengthened using CFRP ropes as external reinforcement," Eng Struct, vol. 250, Jan. 2022, doi: 10.1016/j.engstruct.2021.113305.

Y. T. Obaidat, G. A. F. R. Abu-Farsakh, and A. M. Ashteyat, "Retrofitting of partially damaged reinforced concrete beam-column joints using various plate-configurations of CFRP under cyclic loading," Constr Build Mater, vol. 198, pp. 313-322, Feb. 2019, doi: 10.1016/j.conbuildmat.2018.11.267.

D. Mostofinejad and M. Hajrasouliha, "3D beam-column corner joints retrofitted with X-shaped FRP sheets attached via the EBROG technique," Eng Struct, vol. 183, pp. 987-998, Mar. 2019, doi: 10.1016/j.engstruct.2019.01.038.

G. L. Wang, J. G. Dai, and Y. L. Bai, "Seismic retrofit of exterior RC beam-column joints with bonded CFRP reinforcement: An experimental study," Compos Struct, vol. 224, Sep. 2019, doi: 10.1016/j.compstruct.2019.111018.

S. Alavi-Dehkordi, D. Mostofinejad, and P. Alaee, "Effects of high-strength reinforcing bars and concrete on seismic behavior of RC beam-column joints," Eng Struct, vol. 183, pp. 702-719, Mar. 2019, doi: 10.1016/j.engstruct.2019.01.019.

A. Marchisella, G. Muciaccia, A. Sharma, and R. Eligehausen, "Experimental investigation of 3d RC exterior joint retrofitted with fully-fastened-haunch-retrofit-solution," Eng Struct, vol. 239, Jul. 2021, doi: 10.1016/j.engstruct.2021.112206.

H. Behnam, J. S. Kuang, and R. Y. C. Huang, "Exterior RC wide beam-column connections: Effect of beam width ratio on seismic behaviour," Eng Struct, vol. 147, pp. 27-44, Sep. 2017, doi: 10.1016/j.engstruct.2017.05.044.

Y. R. Dong, Z. D. Xu, Q. Shi, Q. Q. Li, Z. H. He, and Y. Cheng, "Seismic performance and material-level damage evolution of retrofitted RC framed structures by high-performance sAVED under different shear-span ratio," Journal of Building Engineering, vol. 63, Jan. 2023, doi: 10.1016/j.jobe.2022.105495.

Q. Huang, Y. Liu, and L. Tian, "Seismic performance of the shear-deficient exterior RC beam-column joints strengthened with PHSW," Eng Struct, vol. 275, p. 115309, Jan. 2023, doi: 10.1016/J.ENGSTRUCT.2022.115309.

H. Wang, H. Huang, Y. Cheng, Y. Dai, and L. Zhang, "Experimental and numerical investigation on strengthening mechanism of rib-reinforced round-over-round RCFDST column jointed with steel beam under cyclic loading," Thin-Walled Structures, vol. 192, Nov. 2023, doi: 10.1016/j.tws.2023.111049.

M. Kwon, Y. Jeong, and J. Kim, "Numerical Study of RC Beam-Column Joints Using a 4-Node Lattice Element Analysis Method," KSCE Journal of Civil Engineering, vol. 25, no. 3, pp. 960-972, Mar. 2021, doi: 10.1007/s12205-021-0991-z.

R. Ganasan, C. G. Tan, Z. Ibrahim, F. M. Nazri, M. M. Sherif, and A. El-Shafie, "Development of crack width prediction models for rc beam-column joint subjected to lateral cyclic loading using machine learning," Applied Sciences (Switzerland), vol. 11, no. 16, Aug. 2021, doi: 10.3390/APP11167700.

"318M-19: Building Code Requirements for Structural Concrete and Commentary, Metric." Accessed: Dec. 23, 2025. [Online]. Available: https://www.concrete.org/publications/internationalconcreteabstractsportal.aspx?m=details&id=51722448